

Chris J. Peterson\*

University of Georgia, Athens, Georgia

Christopher M. Godfrey

University of North Carolina at Asheville, Asheville, North Carolina

Franklin T. Lombardo

University of Illinois at Urbana–Champaign, Urbana, Illinois

Jeffery B. Cannon†

University of Georgia, Athens, Georgia

## 1. INTRODUCTION

An important but poorly-resolved question in studies of tornado formation and behavior is how much geomorphic, vegetation, or other non-atmospheric environmental conditions influence tornado characteristics such as formation, movement, and duration (Schenkman et al. 2014; Roberts et al. 2016). A number of empirical studies have examined the influence of large-scale topographic variability on various aspects of tornado formation or behavior for tracks that traverse ridges, mountains, or valleys (e.g., LaPenta et al. 2005; Bosart et al. 2006; Lyza and Knupp 2014; Cannon et al. 2016), although numerical modeling studies that incorporate topographic influences have been much rarer (e.g., Lewellen 2012; Markowski and Dotzek 2011). Nevertheless, both empirical and modeling studies repeatedly confirm the potential for complex terrain to influence tornado behavior.

Fine-scale surface roughness may, however, influence tornado behavior via distinct mechanisms. In particular, coarse-scale features such as ridges or valleys obviously remain immovable, while strong winds may knock down fine-scale features such as trees or small structures, which no longer impede winds more than a few meters above the surface. Moreover, while the wind cannot penetrate large-scale topographic features, some fine-scale features such as trees may be at least partially porous to tornadic winds. Notably, existing numerical modeling or simulation studies include rigid, widely-spaced idealized structures (Lewellen 2012) or a stated amount of surface drag induced by unspecified sources (e.g., Schenkman et al. 2012; Roberts et al. 2016). The present work aims to provide empirical specificity to complement existing simulation studies. While this effort does not examine tornado dynamics directly, the calculations herein generate real-world estimates of drag, torque, and energy dissipation from actual tornadoes in heavily-forested land-

scapes. This work is also distinct from a variety of recent studies—often motivated by the pioneering early work of Letzmann (1923) and later Holland et al. (2006)—that have used forest and tree damage patterns to retrospectively infer tornado characteristics (e.g., Beck and Dotzek 2010; Bech et al. 2009; Karstens et al. 2013; Kuligowski et al. 2014).

Simulation studies by Schenkman et al. (2014) and Roberts et al. (2016) point out the unexpectedly large influence of surface roughness during tornadogenesis. Yet these studies utilize surface roughness values thought to be representative of farmlands or other land uses of modest roughness. In contrast, the larger and less flexible surface of a forest might be a sink for hundreds or thousands of times more energy than farmlands, with presumably greater potential to influence tornadoes. In light of this, Forbes (1998) estimates that a 31 May 1985 tornado in Pennsylvania snapped or uprooted as many as 1000 trees per second at its widest point. These findings provide a strong motivation for empirical work that explores the drag imposed on a vortex by surface features, as well as the force exerted by the tornado and the mechanical work accomplished. Might the drag or torque imposed by the forest—or the force expended in overturning trees—be sufficient to influence tornadic winds? The answer is surely unknown at this time, but in an effort to quantify the magnitude of such effects, the present work presents estimates of four quantities calculated at regular intervals along two tornadoes that moved across heavily forested, complex terrain in the southern Appalachians: drag and torque exerted by the forest on the vortex, the force exerted by the wind in the process of overturning the trees, and the mechanical work accomplished by overturning the trees.

## 2. DATA

Two long-track tornadoes that occurred as part of the 27 April 2011 tornado outbreak passed over heavily-forested areas in the southeastern United States. One tornado passed through the Chattahoochee National Forest (CNF) in northeastern Georgia, carving a continuous swath of damage over 58.3 km east-northeastward across

---

\*Corresponding author address: Chris J. Peterson, University of Georgia, Department of Plant Biology, 2502 Miller Plant Sciences, Athens, Georgia 30602; e-mail: cjpete@uga.edu.

†Current affiliation: Colorado Forest Restoration Institute, Colorado State University, Fort Collins, Colorado.

Lumpkin, White, Habersham, and Rabun Counties and finally lifting just east of Mountain City, GA. A National Weather Service (NWS) damage survey team assigned an EF3 rating to the tornado. The second tornado passed through the Great Smoky Mountains National Park (GSMNP) in eastern Tennessee, carving a 26.0-km swath of damage through the extreme western side of the national park. The tornado touched down in eastern Monroe County, TN and tracked east-northeastward through Blount County, lifting near the northwestern park boundary just west of Townsend, TN. Based on a single damage indicator just outside of the national park, a NWS damage assessment team assigned a rating of EF4 to this tornado.

## 2.1 Characterization of damage

Sixty-four days after the tornado outbreak, a chartered flight captured vertical aerial photographs along the entire length of both tornado tracks, with a nominal pixel resolution of 20 cm (8 inches). These high-resolution, georeferenced images show individual tree trunks, crowns, and root balls. Both Cannon (2015) and Cannon et al. (2016) fully describe the details of the imagery analysis via GIS software. These GIS analyses quantify the spatial variation in forest damage severity along the same tornado tracks studied here, while also providing estimates of damage track width (Cannon et

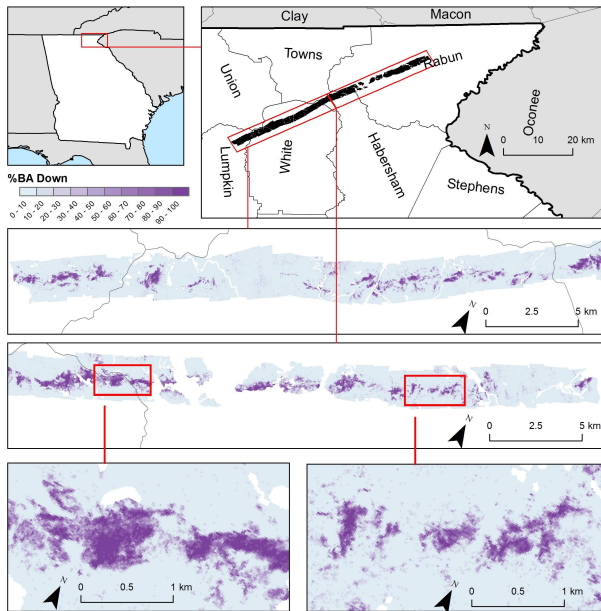


FIG. 1. Map showing the damage path and severity of forest damage for the 27 April 2011 Chattahoochee National Forest tornado. The top panel and inset show the location of the damage path in the state of Georgia. The two middle panels, representing the western and eastern halves of the tornado track, show the variation in damage patch size, shape, and severity. The bottom insets show two representative portions of the damage path. Note that the middle and lower panels have been rotated to conserve space. From Cannon et al. (2016).

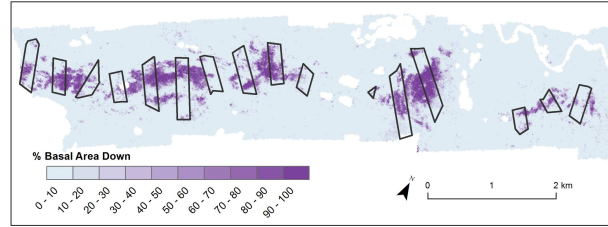


FIG. 2. Graphical representation of the locations and shapes of samples at 500-m intervals along the first (western) 8.5 km of the CNF tornado track. Samples run a length of 200 m parallel to the tornado path with a perpendicular dimension corresponding with the width of contiguous forest damage that exceeds 15% of basal area down. From Cannon et al. (2016).

al. 2016). A supervised classification algorithm (Lillesand et al. 2015) quantifies the forest damage severity. Several hundred training plots measuring  $20\text{ m} \times 20\text{ m}$  and distributed randomly over the length of each tornado track ( $n = 1200$  for CNF and  $n = 670$  for GSMNP) allow a visual classification of both damaged and undamaged forest into five damage severity categories (none, low, medium, high, and very high) that roughly correspond with the proportion of the forest canopy removed by the tornado. Spectral signatures derive from the training plots following a resampling process that reduces the resolution of the imagery to  $4\text{ m pixel}^{-1}$  to mitigate the unwanted influence of shadows and individual trees. GIS software then classifies each pixel of the remaining imagery into one of the five damage levels. Averages of the damage severity of adjacent pixel clusters yield an estimate of damage severity for  $20\text{ m} \times 20\text{ m}$  cells across the entire damage track for each tornado (Fig. 1). Correlation analyses confirm that the damage severity, quantified as the proportion of the forest canopy removed by the tornado, is proportional to the percentage of basal area (a cumulative measure of the sum of all tree trunk areas in a given plot) down (Cannon et al. 2016). Therefore, canopy damage severity serves as a surrogate for the percentage of basal area down.

Following the development of the damage map in Fig. 1, selected points at 500-m intervals along the subjective centerline of each tornado track serve as beginning locations for each damage path segment. These segments run a length of 200 m parallel to the tornado path with a dimension perpendicular to the tornado path that includes all contiguous pixels with estimated damage in excess of 15% (Fig. 2). The removal of isolated, outlying patches of damage smaller than 8 pixels ( $3200\text{ m}^2$ ) reduces noise in the damage pattern. Each damage track segment receives an assigned value of the average severity of damage (i.e., the mean percentage of basal area down) and a damage swath width.

## 2.2 Tree wind resistance, mass, and center of mass

Peterson and Claassen (2013) and Cannon et al. (2015) perform empirical tree winching experiments to measure

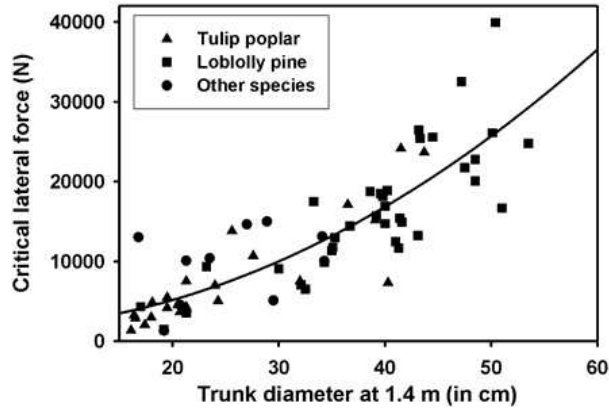


FIG. 3. Critical lateral force (in Nm) necessary to overturn trees as a function of trunk diameter at 1.4 m (dbh) based on 69 trees overturned in a static winching study in central Georgia.

the force necessary to overturn trees of various sizes and species through either trunk breakage or uprooting. Such experiments employ a winch and cable system, with one end attached to the base of an “anchor tree” and the other end attached roughly one-half to two-thirds up the central trunk of a “pulled tree”. The winch increases the force until the pulled tree fails via trunk breakage or uprooting. A load cell positioned between the cable and the pulled tree measures the critical force necessary to overturn the tree. The highest recorded force during the winching process is considered the critical force, and is typically reached when the trunk has been pulled 5–15 degrees from vertical. The critical force measured by the load cell is decomposed into vertical and horizontal components, and the critical horizontal component is considered to be representative of the horizontal force that would be necessary for the horizontal wind to cause tree failure. Trunk diameter strongly influences the critical horizontal force (Fig. 3), but both Peterson and Claassen (2013) and Cannon et al. (2015) report no difference in critical horizontal force between tree species when controlling for trunk diameter. Therefore, the present analyses use regression equations developed with all species pooled in order to predict the critical horizontal force based on tree size, where the standard measurement in forestry and ecology for tree size is the trunk diameter at 1.4 m above the ground, called diameter at breast height (dbh). Tree stability (i.e., the force necessary to overturn the tree) increases in a positive quadratic fashion with tree size, and with little difference among species, as shown in Fig. 3 (Cannon et al. 2015).

Winching experiments primarily quantify the critical turning moment at the base of the tree, which requires information on the vertical center of mass for each pulled tree. Both Peterson and Claassen (2013) and Cannon et al. (2015) cut pulled trees into 1-m sections and either directly weighed them or measured their length and diameter and calculated their weight based on volume and density. Calculations for the change in potential energy, and

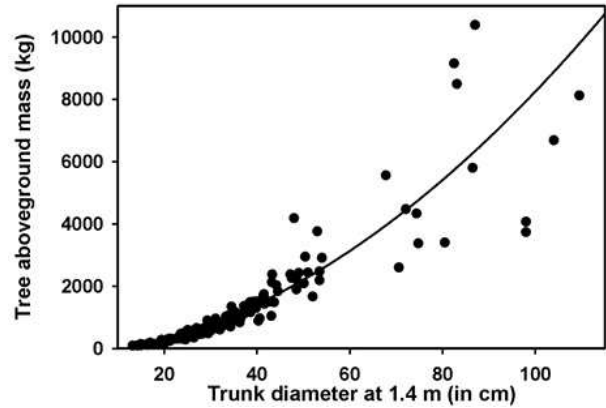


FIG. 4. Aboveground mass of trees as a function of trunk diameter at 1.4 m (dbh) based on two static winching studies on 141 trees of numerous species.

thus work accomplished, ultimately require estimates of the total mass and vertical center of mass for each tree in the damage track segments in the present study. Statistical predictions of total mass as a function of dbh for these trees rely on total mass data based on 141 trees of numerous species in the two Peterson and Claassen (2013) and Cannon et al. (2015) winching studies (Fig. 4). Estimates for the vertical center of mass for each pulled tree in the winching studies derive from the cumulative mass of 1-m trunk sections, beginning from ground level, up to a height where the cumulative mass is equal to half the mass of the whole tree. Predictions of the height of the center of mass as a function of dbh allow predictions of the vertical center of mass for ideal trees in the present analysis. Tree total height is based on field surveys from a tornado blowdown study in northeastern Pennsylvania, in which total height was measured along with trunk dbh for 754 trees. These tree heights and dbh values help to

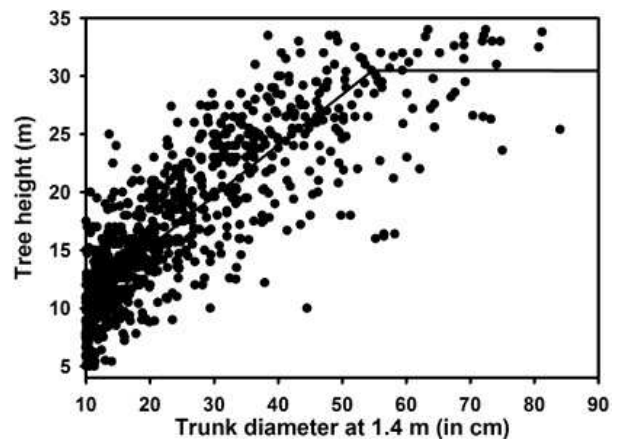


FIG. 5. Tree height as a function of trunk diameter at 1.4 m (dbh) based on 754 trees of numerous species measured in damage survey plots following a tornado in northeastern Pennsylvania. Tree heights for trees with dbh in excess of 55 cm are assumed constant.

determine a regression relationship that is limited to trees with dbh between 10 and 55 cm. Larger-diameter trees are assigned a constant height of 31 m (Fig. 5). These regression equations provide estimates of the total tree mass and the vertical center of mass for the set of ideal trees with diameters at the midpoints of the 10-cm diameter size classes.

### 2.3 Tree density and size structure

Field damage surveys conducted in the two tornado tracks during the summers of 2011–13 yield data on the spatial density of trees and the relative abundance of trees across 10-cm dbh size classes. These field damage surveys also provide ground truth data that confirm the reliability of the GIS-based estimates of damage severity (Cannon et al. 2016). A total of 65 surveys took place within the CNF track, with each sample plot measuring 20 m × 20 m and with plots clustered in three separate locations approximately 15 km apart. A total of 22 surveys took place within the GSMNP track, spread along several km along the long axis of the tornado track. Each survey collected information on the tree species identity, trunk diameter (dbh), type of damage (i.e., standing or fallen), and treefall orientation for every tree in excess of 10 cm dbh. The density and tree size structure revealed in these damage surveys presumably represents the characteristics of each forest along the entire tornado track. The total of all surveyed trees divided by the total sampled ground area allows a measure of the average tree density for each forest, expressed in units of hectare<sup>-1</sup> (ha<sup>-1</sup>).

Field damage surveys reveal nearly identical mean tree densities in the two tornado tracks, with a density of 567.5 trees ha<sup>-1</sup> in the CNF plots and 572.5 trees ha<sup>-1</sup> in the GSMNP plots. The size distribution of trees is also very similar between the two tornado tracks (Table 1). At 48.0% and 44.6% in the CNF and GSMNP tracks, respectively, the greatest fraction of trees by far appear in the smallest size class of 10–19.9 cm dbh, with a steadily decreasing fraction of trees appearing in larger size classes. The largest two size classes of 80–89.9 dbh and more than 90.0 cm dbh each contain less than 1% of the total number of trees.

## 3. APPROACH

This effort aims to produce estimates of four quantities in small segments along each of the two tornado tracks: drag, torque, force exerted in toppling trees, and mechanical work accomplished. These estimates draw upon three sources of background information: 1) winching studies that measure the horizontal force necessary to overturn trees and that also provide total mass and center of mass information as a function of tree size (Peterson and Claassen 2013; Cannon et al. 2015); 2) GIS studies that define the damage width and severity levels within small segments of the damage path for the two tornadoes

TABLE 1. Tree size distributions observed in ground survey plots in the Chattahoochee National Forest (CNF) and the Great Smoky Mountains National Park (GSMNP) within two tornado tracks. Tree size is measured as trunk diameter at 1.4 m above ground (dbh) in cm.

Size class (cm)	CNF		GSMNP	
	Trees	Percentage	Trees	Percentage
10.0–19.9	708	48.0%	194	44.6%
20.0–29.9	323	21.9%	114	26.2%
30.0–39.9	219	14.8%	67	15.4%
40.0–49.9	121	8.2%	34	7.8%
50.0–59.9	55	3.7%	13	3.0%
60.0–69.9	29	2.0%	6	1.4%
70.0–79.9	11	0.7%	5	1.1%
80.0–89.9	7	0.5%	2	0.5%
> 90.0	2	0.1%	0	0.0%
Total	1475	100.0%	435	100.0%

studied here (Cannon et al. 2016); and 3) ground surveys that provide information on the typical spatial density and size structure of trees within the damage tracks. The ground surveys, then, provide information on the relative abundance of trees across 10-cm dbh size classes.

Since calculations for the four quantities vary with tree size, ideal trees with diameters that correspond to the midpoint of each 10-cm dbh size class (e.g., 15 cm, 25 cm, etc.) help to avoid separate calculations for every possible tree size. Each ideal tree receives an estimate of each of the four quantities and the values are summed across the number of trees for each size class in each track segment. **Drag** (in newtons) is calculated for a variety of wind speeds. Calculation of drag at any given wind speed, detailed below, requires knowledge of the wind speed, tree crown lateral area, air density, and a drag coefficient. **Torque** (in newton-meters) from the forest acting on the tornado vortex is a product of the drag and the distance from the center of the vortex to each tree. **Mechanical work accomplished** (in joules) in each damage track segment corresponds with the cumulative pre-storm potential energy for all **fallen** trees. Here, the potential energy of position depends on the total mass and height of the center of mass of each tree, which then presumably drops to zero when the tree falls to the ground. Based on the results of winching studies, the total **force** (in newtons) exerted on the forest is the critical horizontal force necessary to cause failure of a tree in a given size class, summed across all fallen trees in a damage track segment.

## 4. TARGET QUANTITIES

### 4.1 Overturned trees per segment

The damage track segment area and tree density allow an estimate of the total number of trees in each segment. Binning the trees by 10-cm size classes according to the relative frequencies of tree sizes from the field damage surveys yields an estimate of the number of overturned

TABLE 2. Example calculations for two tornado path segments. For each segment,  $n_{\text{trees}}$  gives the estimated number of standing trees in each size class (cm dbh) prior to the wind disturbance ( $s$ ) and the number overturned by the tornado ( $f$ ),  $F_{d_{25}}$  is the surface drag (kN) at a wind speed of  $25 \text{ m s}^{-1}$ , again both before ( $s$ ) and after ( $f$ ) trees overturn,  $\Delta\text{PE}$  is the change in potential energy (MJ), and  $F_T$  is the total force (kN) necessary to overturn the trees.

Size class (cm)	$n_{\text{trees}}$ (s/f)	$F_{d_{25}}$ (s/f)	$\Delta\text{PE}$	$F_T$
CNF Segment 109				
10.0–19.9	886 / 0	972.6 / 972.6	0.0	0.0
10.0–19.9	886 / 0	972.6 / 972.6	0.0	0.0
20.0–29.9	404 / 0	786.4 / 786.4	0.0	0.0
30.0–39.9	273 / 0	832.5 / 832.5	0.0	0.0
40.0–49.9	151 / 0	654.0 / 654.0	0.0	0.0
50.0–59.9	68 / 31	394.5 / 250.6	13.8	956.7
60.0–69.9	37 / 37	245.2 / 49.0	26.5	1580.4
70.0–79.9	13 / 13	97.0 / 19.4	14.0	735.4
80.0–89.9	9 / 9	74.6 / 14.9	13.8	651.9
≥90.0	2 / 2	18.2 / 3.6	4.2	180.6
Total	1845 / 92	4075 / 3583	72.5	4105
GSMNP Segment 15				
10.0–19.9	7968 / 0	8746 / 8746	0.0	0.0
20.0–29.9	4682 / 0	9114 / 9114	0.0	0.0
30.0–39.9	2753 / 0	8395 / 8395	0.0	0.0
40.0–49.9	1395 / 0	6042 / 6042	0.0	0.0
50.0–59.9	537 / 156	3115 / 2391	69.7	4814
60.0–69.9	250 / 250	1657 / 331	179.2	10 678
70.0–79.9	197 / 197	1470 / 294	211.4	11 144
80.0–89.9	91 / 91	754 / 151	139.1	6591
≥90.0	0 / 0	0 / 0	0.0	0.0
Total	17 869 / 693	39 294 / 35 464	598.1	33 228

trees by size class in each segment (Table 1). The damage severity estimated for that segment defines the level of damage in terms of percentage of basal area down. When severe winds impact forests, the largest trees consistently have a higher probability of falling than smaller trees (Everham and Brokaw 1996; Peterson 2007). The calculation of the number of overturned trees per segment therefore proceeds by progressively removing trees from larger to smaller size classes until the treefall percentage matches the necessary percentage of basal area down. Table 2 illustrates calculations of the target quantities for two segments, one small and one large. For example, the damage area within CNF segment 109 is  $3.25 \text{ ha}$ . The overall tree density of  $567.5 \text{ trees ha}^{-1}$  yields an estimate of 1845 trees prior to the wind disturbance. The mean damage severity within this segment is 25.2%, so trees are removed progressively beginning with the largest size classes until reaching the same percentage of the basal area. The pre-disturbance basal area in this segment is  $126.5 \text{ m}^2$ , of which 25.2% is  $31.8 \text{ m}^2$ . The two trees with diameters in excess of 90 cm each contribute a basal area of  $\pi \left(\frac{95 \text{ cm}}{2}\right)^2 = 0.709 \text{ m}^2$  for a total of  $1.418 \text{ m}^2$  of basal area. The nine trees in the 80–89.9 cm size class each contribute  $0.567 \text{ m}^2$  for a total of  $5.103 \text{ m}^2$  of basal area. This accumulation continues through the 70–79.9 and 60–69.9 cm size classes, which contribute  $5.743 \text{ m}^2$  and  $12.278 \text{ m}^2$  of basal area, respectively. Therefore,

by assuming that all trees with diameters of 60 cm or more fall during the tornado, the total basal area down sums to  $24.542 \text{ m}^2$ . This total is less than  $31.8 \text{ m}^2$  and implies that some of the 50–59.9 cm trees must also fall. Cumulatively, all of the 50–59.9 cm dbh trees would contribute  $16.184 \text{ m}^2$  of basal area, overshooting the target of  $31.8 \text{ m}^2$ . Adding 31 trees from the 50–59.9 cm dbh size class brings the rounded total to  $31.8 \text{ m}^2$ . Consequently, this approach provides an estimate of 92 overturned trees within this segment. The same procedure gives an estimate of 17 869 trees within the larger segment GSMNP 15 in which the damage severity is 21.4%, or  $258.208 \text{ m}^2$  blown down. Summing the basal area of all trees with sizes of 60.0 cm dbh or more yields  $221.618 \text{ m}^2$ , so the target is reached by adding 156 trees from the 50–59.9 cm dbh size class. Therefore, a total of 694 trees fell within the GSMNP 15 segment (Table 2).

## 4.2 Change in potential energy

The gravitational potential energy associated with the pre-disturbance position of a tree in each ideal tree size category is  $mgh$ , where  $m$  is the total aboveground mass (kg),  $g = 9.8 \text{ m s}^{-2}$  is the acceleration of gravity, and  $h$  is the height of the center of mass (m). Assuming the center of mass of each fallen tree is at a height of zero meters, the total change in potential energy following the tornado, and hence mechanical work accomplished, is equivalent to the pre-disturbance potential energy summed across the number of trees in each ideal size class.

## 4.3 Total drag per segment

Drag on a given tree is given by

$$F_d = \frac{1}{2} C_d A_s \rho V^2, \quad (1)$$

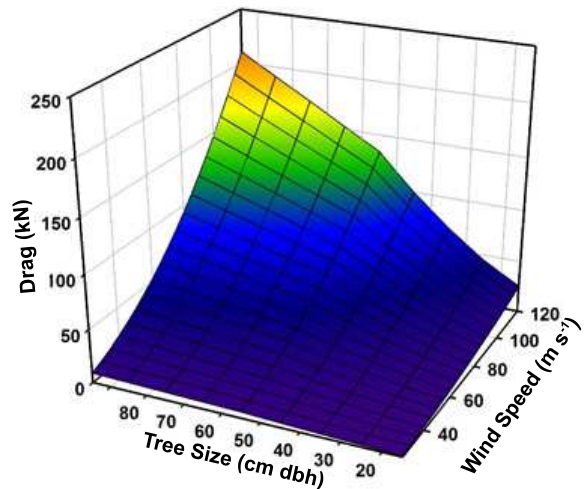


FIG. 6. Drag on trees of different sizes at a variety of wind speeds given in  $5 \text{ m s}^{-1}$  intervals from  $25\text{--}120 \text{ m s}^{-1}$ .

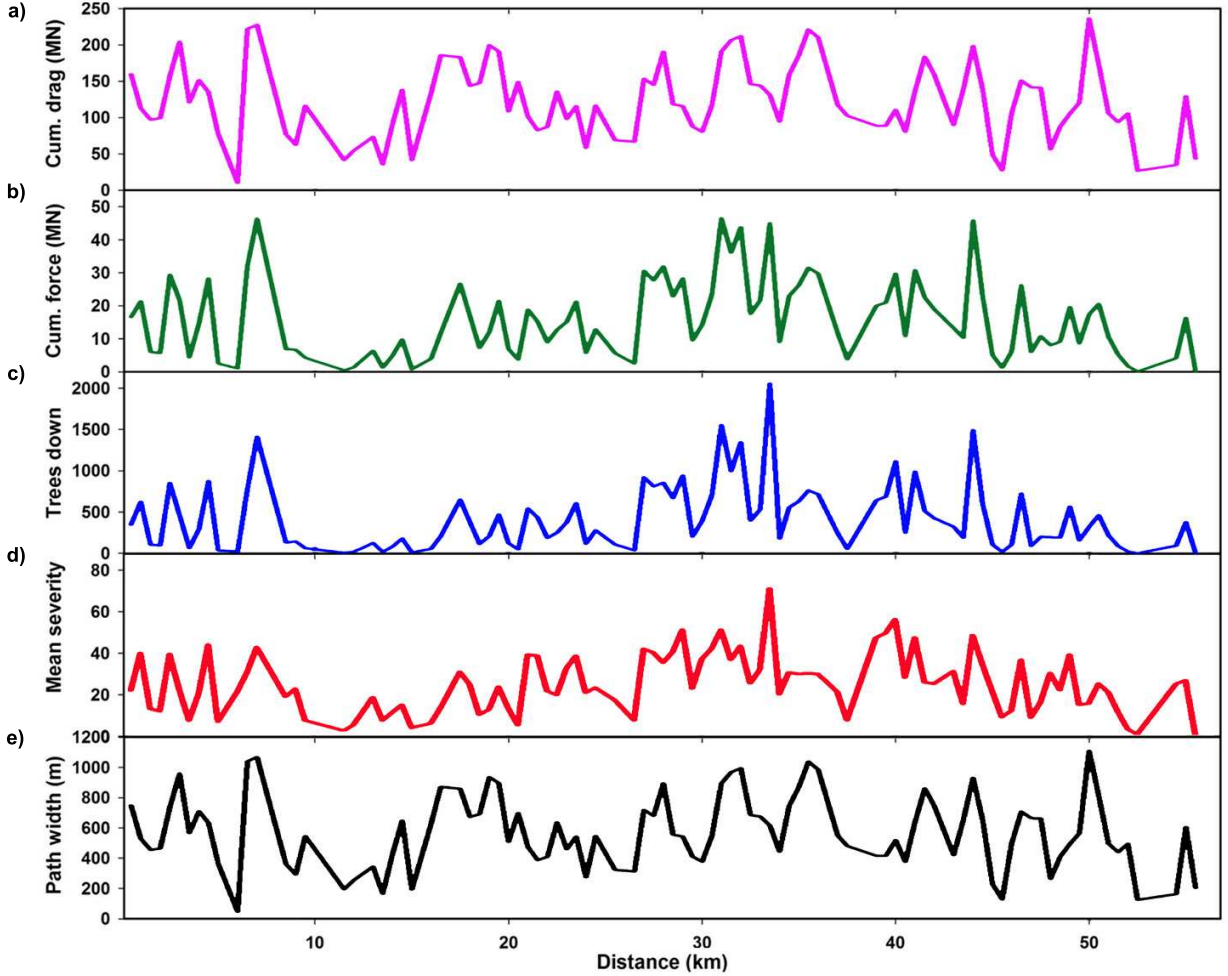


FIG. 7. Spatial variation of a) cumulative drag (MN) on the vortex, b) cumulative force (MN) exerted in the process of overturning trees, c) the number of overturned trees, d) the mean damage severity (given as the percentage of basal area down), and e) the path width (m) along the path of the CNF tornado. Each point corresponds with one of 93 samples along the entire tornado track.

where  $F_d$  is the drag force (N),  $C_d$  is a dimensionless drag coefficient,  $A_s$  is the streamlined (see below) area of the tree ( $\text{m}^2$ ),  $\rho = 1.1 \text{ kg m}^{-3}$  is the air density, and  $V$  is the wind speed ( $\text{m s}^{-1}$ ) (Peltola 2006). Here,  $C_d = 1.0$  for tree trunks and  $C_d = 0.29$  for tree crowns following Holland et al. (2006). Fig. 6 illustrates the drag on trees of different sizes at a variety of wind speeds given in  $5 \text{ m s}^{-1}$  intervals from  $25$ – $120 \text{ m s}^{-1}$ . Tree crowns also bend and deform, or streamline, under the influence of high winds (Holland et al. 2006; Beck and Dotzek 2010). To account for streamlining, the still-air tree crown area is reduced by 60% for all wind velocities in excess of  $20 \text{ m s}^{-1}$  following Holland et al. (2006). The average deflection from vertical for winched trees corresponds with a maximum turning moment of  $12.2^\circ$  from vertical (Peterson and Claassen 2013; Cannon et al. 2015). To realistically model bending, the still-air tree height is therefore reduced by a factor of  $\cos 12.2^\circ$ . Calculations for both drag and torque rely on the dimensions of these bent and streamlined trees.

#### 4.4 Torque

The drag imposed by trees is of course not all applied at the same distance from the center of the vortex, so a calculation of torque based on the distance of a tree from the center of rotation may be more informative. Torque in newton-meters (Nm) is given by

$$\tau = r_b F_d, \quad (2)$$

where  $r_b$  is the distance of the tree from the center of the tornado vortex (m). Though geographic coordinates are available for each standing and fallen tree in both tornado tracks (Godfrey and Peterson 2016), a simpler and more straightforward approach involves making a reasonable approximation for the number of trees located in bands at different distances from the center of rotation and calculating  $\tau$  within those distance bands for a selection of possible wind speeds. Since the tornadoes under study here moved predominantly eastward, the damage track

TABLE 3. Damage swath characteristics for sample segments along the CNF and GSMNP tornado tracks.

	CNF	GSMNP
Number of segments	93	51
Damage severity by segment		
Min-Max	0.6–71.1	5.9–64.5
$\bar{x} \pm \sigma$	$25.2 \pm 14.4$	$26.2 \pm 12.6$
Swath width (m) by segment		
Min-Max	46–1109	226–1645
$\bar{x} \pm \sigma$	$572.6 \pm 244.4$	$953.4 \pm 321.3$
Pre-event standing trees by segment		
Min-Max	524–12 586	2587–18 838
$\bar{x} \pm \sigma$	$6499 \pm 2774$	$10 917 \pm 3679$
Post-event overturned trees by segment		
Min-Max	1–2056	39–2303
$\bar{x} \pm \sigma$	$415 \pm 404$	$618 \pm 439$
Force expended by segment (kN)		
Min-Max	90–46 564	2412–51 926
$\bar{x} \pm \sigma$	$15 685 \pm 11 885$	$24 006 \pm 11 634$
Mechanical work accomplished by segment (MJ)		
Min-Max	2.1–709	47.8–731
$\bar{x} \pm \sigma$	$259.4 \pm 176.3$	$401.9 \pm 171.6$
Cumulative force expended in all segments (MN)	1459	1224
Cumulative force expended for entire track (MN)	4567	3121
Cumulative work accomplished in all segments (MJ)	24 123	20 498
Cumulative work accomplished in entire track (MJ)	75 505	52 270

width in each segment is partitioned into east-west bands such that each band covers 20% of the damage track in that segment. The innermost band 1 straddles the centerline. Bands 2 through the outermost band 5 are split into northern and southern halves, with the lower-numbered bands nested between the halves of the higher-numbered bands. Assuming a random distribution of trees relative to the centerline of each segment, 20% of the total drag  $F_d$  in each segment is assigned to each of bands 1–5 for each possible wind speed. The distance  $r_b$  is then the mean distance from the centerline for each band. For example, the total width of the damage in segment CNF 109 is  $w = 162.6$  m, giving a distance of 81.3 m from centerline to the edge of the damage path. The distance from the centerline to the outer edge of this innermost band covers one fifth of this distance and is therefore 16.26 m on either side of the centerline. The mean distance from the centerline to band 1 is therefore  $r_{b_1} = 8.13$  m. Just outside band 1, the region from 16.26 m to 32.52 m on either side of the centerline defines band 2. The mean distance from the centerline for band 2 is therefore  $r_{b_2} = 24.39$  m and so on. Similarly, segment GSMNP 15 has a damage track width of  $w = 1560.6$  m, giving  $r_{b_1} = 78.03$  m,  $r_{b_2} = 156.06$  m, and so on out to  $r_{b_5}$ . Therefore, the torque for each segment within band  $n$  is  $\tau_n = 0.2F_d r_{b_n}$ , evaluated for each possible wind speed.

Note that these calculations of drag and torque assume a constant vertical wind profile from the surface through the height of the trees. Rare Doppler radar observations of tornadic winds very near to the surface reveal that winds often maintain a linear velocity profile down to 2–3 m above ground level (J. Wurman, personal communication). Even if the calculations were to assume a non-uniform wind profile, the characteristics of that ver-

tical profile remain unclear. Therefore, the authors have chosen to use a uniform vertical wind profile here, despite the assumption of a logarithmic profile as used by Holland et al. (2006) and Beck and Dotzek (2010).

## 5. RESULTS

The selection of segments from the damage map along each tornado track yields a total of 144 segments, with 93 in the CNF track and 51 in the GSMNP track. Although the damage along both tornado tracks is discontinuous, with undamaged patches interspersed within the primary damage path (Cannon et al. 2016), there remains considerable variability in the width of the damaged regions within segments with measurable damage (Fig. 7). These damage widths range from less than 50 m to over 1600 m (Table 3). The damage track is generally wider for the GSMNP tornado, averaging approximately 950 m, compared with the average damage width of approximately 572 m in the CNF tornado track. Similarly, the mean damage severity varies substantially among segments, ranging from less than 1% to more than 70% basal area down (Fig. 7; Table 3). The mean damage severity, however, is nearly identical for both tornado tracks. These summary measures do not fully characterize the variation in severity. Personal observations by the authors reveal that many damaged patches experienced essentially 100% canopy destruction, but do not exactly coincide with the boundaries of the segments reported here. Due to the large variability of damage path width along each tornado track, the number of pre-disturbance trees standing in each segment varies considerably (Fig. 7). The combination of varying path width and damage severity

TABLE 4. Pre-storm drag (MN) from standing trees.

Velocity ( $\text{m s}^{-1}$ )	CNF		GSMNP	
	Min-Max	Mean $\pm$ S.D.	Min-Max	Mean $\pm$ S.D.
25	1.1–27.8	14.4 $\pm$ 6.1	5.7–41.4	23.9 $\pm$ 8.2
30	1.7–40.0	20.7 $\pm$ 8.8	8.2–59.6	34.5 $\pm$ 11.7
35	2.3–54.5	28.2 $\pm$ 12.0	11.1–81.2	46.9 $\pm$ 16.0
40	3.0–71.2	36.8 $\pm$ 15.7	14.6–106.0	61.2 $\pm$ 20.9
45	3.8–90.1	46.6 $\pm$ 19.9	18.4–134.2	77.5 $\pm$ 26.4
50	4.7–111.3	57.5 $\pm$ 24.5	22.7–165.6	95.7 $\pm$ 32.6
55	5.7–134.6	69.5 $\pm$ 29.7	27.5–200.4	115.8 $\pm$ 39.5
60	6.7–160.2	82.8 $\pm$ 35.3	32.8–238.5	137.8 $\pm$ 47.0
65	7.9–188.1	97.1 $\pm$ 41.4	38.4–279.9	161.8 $\pm$ 55.1
70	9.2–218.1	112.6 $\pm$ 48.1	44.6–324.6	187.6 $\pm$ 63.9
75	10.5–250.4	129.3 $\pm$ 55.2	51.2–372.7	215.4 $\pm$ 73.4
80	12.0–284.9	147.1 $\pm$ 62.8	58.2–424.0	245.0 $\pm$ 83.5
85	13.5–321.6	166.1 $\pm$ 70.9	65.7–478.7	276.6 $\pm$ 94.3
90	15.2–360.6	186.2 $\pm$ 79.5	73.7–536.6	310.1 $\pm$ 105.7
95	16.9–401.7	207.5 $\pm$ 88.5	82.1–597.9	345.5 $\pm$ 117.8
100	18.7–445.1	229.9 $\pm$ 98.1	91.0–662.5	382.8 $\pm$ 130.5
105	20.7–490.8	253.4 $\pm$ 108.2	100.3–730.4	422.1 $\pm$ 143.8
110	22.7–538.6	278.2 $\pm$ 118.7	110.1–801.6	463.2 $\pm$ 157.9
115	24.8–588.7	304.0 $\pm$ 129.8	120.3–876.2	506.3 $\pm$ 172.6
120	27.0–641.0	331.0 $\pm$ 141.3	131.0–954.0	551.3 $\pm$ 187.9

explains why the number of overturned trees per segment varies by more than two orders of magnitude between segments (Table 3).

### 5.1 Drag

Total drag, in meganewtons (MN), caused by standing trees prior to treefall varies by approximately 24-fold between the maximum and minimum values for each possible wind speed within the CNF segments (Fig. 7; Table 4). There is substantially less variation in drag force among segments in the GSMNP track, with the maximum roughly seven times greater than the minimum value. At a typical wind speed of  $65 \text{ m s}^{-1}$ , for example, drag varies from 7.9 to 188.1 MN in the CNF track, while in the GSMNP track, drag varies from 38.4 to 279.9 MN. The great majority of the difference between the two tracks appears to derive from the generally wider damage path in the GSMNP track.

An extension of this approach can provide drag estimates for many combinations of wind velocity and track length, as shown in Fig. 8. For example, in a hypothetical tornado through the CNF forest with identical damage widths in each segment, a wind velocity of  $65 \text{ m s}^{-1}$  would result in cumulative drag totals of 4856 MN, 14 568 MN, and 24 280 MN for 10-, 30-, and 50-km damage paths, respectively. The corresponding cumulative drag totals for a hypothetical tornado in the GSMNP forest would be 8087 MN, 24 262 MN, and 40 437 MN for 10-, 30-, and 50-km damage paths, respectively. The wider damage segments in the GSMNP tornado produce substantially greater cumulative drag for all wind velocities and track lengths.

### 5.2 Torque

The estimated torque imposed by the trees prior to treefall varies tremendously among track segments (Table 5), with a 569-fold variation between maximum and minimum values in the CNF track and a roughly 53-fold variation in the GSMNP track. The mean torque across all segments ranges from 4855 meganewton-meters (MNm) at a wind speed of  $25 \text{ m s}^{-1}$  to 111 852 MNm at  $120 \text{ m s}^{-1}$  in the CNF track and from 12 689 MNm to 292 342 MNm at the same respective wind speeds in the GSMNP track. For a given wind velocity, the torque is roughly 2.6 times greater in GSMNP segments compared with the CNF segments.

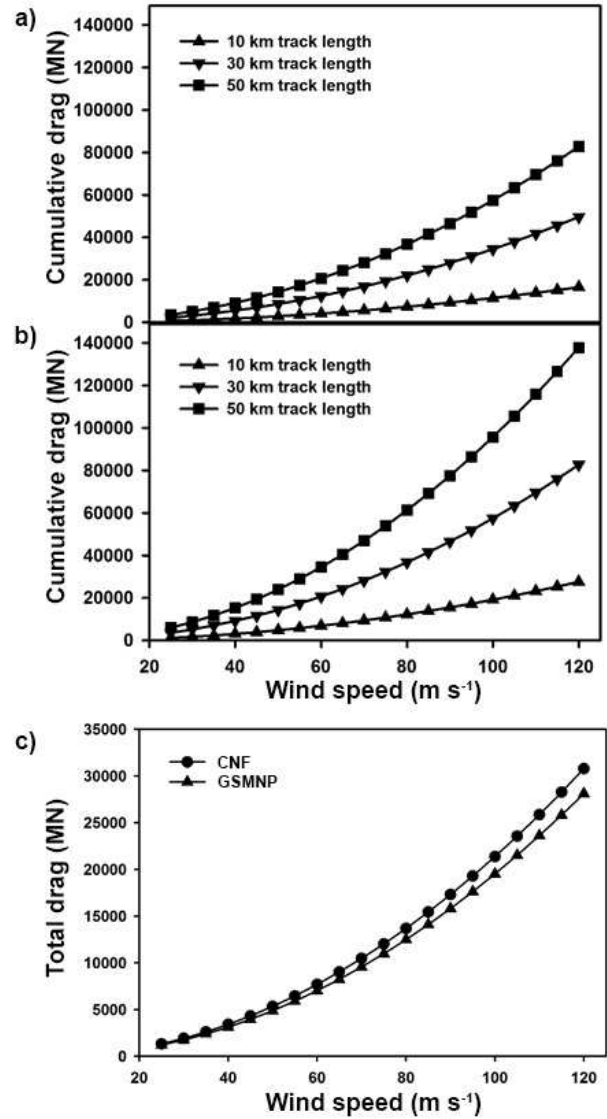


FIG. 8. Cumulative drag (MN) on the tornado vortex as a function of wind velocity for various track lengths in a) the CNF forest and b) the GSMNP forest. Panel c) shows the cumulative drag (MN) as a function of wind velocity in each forest for the observed tornado track lengths.

TABLE 5. Pre-storm torque (MNm) from standing trees.

Velocity (m s <sup>-1</sup> )	CNF		GSMNP	
	Min–Max	Mean ± S.D.	Min–Max	Mean ± S.D.
25	27–15,425	4855 ± 3730	642–34,063	12,689 ± 8232
30	39–22,211	6991 ± 5371	925–49,050	18,271 ± 11,854
35	53–30,232	9515 ± 7311	1259–66,762	24,869 ± 16,135
40	69–39,487	12,428 ± 9548	1644–87,199	32,483 ± 21,074
45	88–49,975	15,729 ± 12,084	2081–110,362	41,111 ± 26,671
50	108–61,698	19,419 ± 14,920	2569–136,249	50,754 ± 32,928
55	131–74,655	23,497 ± 18,053	3108–164,861	61,412 ± 39,843
60	156–88,845	27,963 ± 21,484	3699–196,199	73,086 ± 47,416
65	183–104,269	32,817 ± 25,214	4342–230,258	85,773 ± 55,647
70	212–120,931	38,061 ± 29,243	5035–267,053	99,480 ± 64,539
75	244–138,820	43,692 ± 33,569	5780–306,559	114,196 ± 74,087
80	277–157,947	49,711 ± 38,194	6577–348,796	129,930 ± 84,294
85	313–178,308	56,120 ± 43,118	7424–393,759	146,679 ± 95,161
90	351–199,904	62,918 ± 48,340	8324–441,451	164,444 ± 106,687
95	391–222,729	70,101 ± 53,859	9274–491,856	183,221 ± 118,868
100	433–246,794	77,676 ± 59,679	10,276–544,999	203,017 ± 131,711
105	477–272,090	85,637 ± 65,796	11,329–600,859	223,825 ± 145,211
110	524–298,620	93,987 ± 72,211	12,434–659,466	245,649 ± 159,370
115	573–326,386	102,726 ± 78,925	13,590–720,761	268,490 ± 174,189
120	624–355,381	111,852 ± 85,937	14,798–784,793	292,342 ± 189,663

### 5.3 Force exerted

The total force exerted in the process of overturning trees also varies significantly among individual segments in both tornado tracks (Table 3). The total force exhibits a 500-fold variation within the CNF track, while the GSMNP track exhibits a less-extreme 20-fold variation (Fig. 7). Most of this difference results from the lack of substantial damage in a few of the CNF segments. Conversely, the maximum force exerted in the CNF track is only about 12% greater than the maximum force exerted in the GSMNP track. Averaging across segments within a tornado track, the mean force exerted is roughly 54% greater in the GSMNP track than in the CNF track.

### 5.4 Mechanical work accomplished

The estimate of the mechanical work accomplished as each tornado overturned trees also shows substantial variation among segments within a given tornado track, ranging from 2.1 to 731 MJ, with a pooled average for both tracks of 330.7 MJ per segment (Table 3). Paralleling the force exerted, the variation in work accomplished among segments is roughly 20-fold from the minimum to maximum within the GSMNP track, but nearly 500-fold in the CNF track. The mean work accomplished is 54% greater in the GSMNP tornado.

The cumulative force exerted and mechanical work accomplished in the process of overturning trees can be estimated for the entirety of both tornado tracks by assuming that the damage segments are good representations of their respective tornado damage paths. This is a reasonable assumption given the wide spacing of the segments along both tracks. The regular 500-m interval between segments should mitigate any spatial bias. Linearly extrapolating the 18.6 linear km covered by the 93 sam-

ples in the CNF track to the full 58.3 km of the observed ground damage, and thereby multiplying each estimated quantity by a factor of 3.13, and doing the same for the 10.2 km sampled in the GSMNP track by multiplying by a factor of 2.55 to estimate each quantity for the entire 26.0 km track, reveals the total drag force and mechanical work accomplished by each tornado. The cumulative force exerted on the CNF forest totals slightly more than 4.5 million kN and the mechanical work accomplished is over 75 000 MJ, or the equivalent of 17.9 tons of TNT. The GSMNP tornado exerted slightly more than 3.1 million kN of force on the forest and accomplished approximately 52 000 MJ of mechanical work, or the equivalent of 12.4 tons of TNT. It is worth pointing out that these cumulative totals are somewhat more similar than would be expected on the basis of damage track length alone. The CNF track is 224% of the length of the GSMNP damage track, but the total force exerted on the CNF forest was only 46% greater than the force exerted on the GSMNP forest. Indeed, the average drag force per kilometer by the GSMNP tornado is 120 000 kN km<sup>-1</sup> and only 78 000 kN km<sup>-1</sup> for the CNF tornado. The average mechanical work accomplished per kilometer by the GSMNP tornado is 2010 MJ km<sup>-1</sup> and only 1295 MJ km<sup>-1</sup> for the CNF tornado. Therefore, the GSMNP tornado accomplished 55% more mechanical work per unit length than the CNF tornado. Also noteworthy is the fact that the cumulative mechanical work accomplished by each tornado is roughly similar to the explosive yield of a very small, tactical nuclear weapon such as the Davy Crockett artillery warhead with an explosive yield of 10–20 tons of TNT.

## 6. DISCUSSION

The most striking element to emerge from these analyses is the patchiness of the forest damage created by both tornadoes. Both damage tracks exhibit gaps between the touchdown and end points, with no discernable damage in the remote imagery, with the exception of perhaps slight damage such as defoliation or breakage of small branches. Where the aerial imagery shows detectable damage, both the severity and the damage path width vary tremendously. Indeed, it is difficult to reconcile the spotty impression shown in Figure 1, as well as a similar figure for the GSMNP track in Cannon et al. (2016), with the elongated nested damage polygons that typically emerge from most quantitative tornado damage surveys. It seems likely that some of the difference may lie in the density of points at which surveyors can quantitatively estimate damage severity. In the present study, the density of the trees within both forests allows a separate damage severity estimate for every  $20\text{ m} \times 20\text{ m}$  cell along the entire damage track. In many storm surveys, large spatial gaps may exist between traditional damage indicators that correspond with certain degrees of damage on the enhanced Fujita (EF) scale (WSEC 2006). However, even in the rare cases where surveyors have assigned a degree of damage to nearly every single-family home within a residential area (e.g., Burgess et al. 2014), the spatial variation in damage severity appears substantially less than observed here. Perhaps the very rugged terrain that confronted the two tornadoes studied here may have contributed to the spatial variation in damage severity. For example, Cannon et al. (2016) show clear patterns of increasing forest damage severity as these same tornados traverse downslope, and diminishing severity as they travel upslope, across an enormous variety of terrain.

Though an examination of the relationship between damage path width and severity—which serves as a surrogate for tornado intensity—is not a primary objective of this work, it remains worthwhile to point out that there exists a weak positive correlation ( $r = 0.33$ ) between damage path width and damage severity in the 93 segments of the CNF tornado track, though the 51 segments of the GSMNP track exhibit an even weaker negative correlation ( $r = -0.22$ ). Brooks (2004) reports a weak correlation between width and EF-scale level in an examination of a very large number of tornadoes. In addition, Peterson et al. (2013) find that forest damage patches from a derecho also exhibit a positive correlation between damage patch size and damage severity. Consistent with such findings, it is well known that some of the most damaging EF4 and EF5 tornadoes (e.g., Joplin, MO in 2011 and Moore, OK in 2013) are large wedge tornadoes. Several lines of evidence, therefore, seem to converge on the conclusion that there exists a potential correspondence between tornado intensity and damage path width.

The magnitudes of energy expenditure reported here likely represent only minimal estimates for two rea-

sons. First, there remains no quantitative basis to model the energy expenditure required for partial tree damage, so these estimates consider only the energy required to overturn trees completely. Actual forests, however, can sustain substantial partial tree damage, such as broken branches or partial canopy removal (Peterson 2007), thereby increasing the true energy expenditure over the estimates reported here. Second, results from experimental winching studies have guided the authors' estimates of the force necessary to overturn trees. Winching experiments typically measure the critical force necessary to overturn a tree that does not contact neighboring trees. However, studies have shown that forest trees subjected to high winds may provide substantial mutual support to one another (Rudnicki et al. 2001; Webb et al. 2013), thereby increasing the force necessary to overturn trees that still have standing neighbors. Consequently, the results reported here likely underestimate the true energy expenditure.

Within a given tornado track, it appears that trees in a heavily-forested landscape do indeed present substantial surface roughness. In contrast to tornadoes moving over open farmland or bodies of water, the two tornadoes in this study encountered surface roughness that may have been a sink for hundreds or thousands of times more energy than the smaller and weaker objects that populate agricultural landscapes. Notably, Shenkman et al. (2014) report that the addition of a very modest amount of surface drag to a simulation of the 2013 Moore, Oklahoma tornado alters the dynamics of tornadogenesis through the generation of vertical vorticity near the ground. Similarly, Roberts et al. (2016) find that surface drag enhances vertical vorticity through several mechanisms. Although the present study does not actually quantify surface roughness itself, it does provide a first approximation of the amount of energy that very rough surfaces may absorb from a tornado. Future research efforts might use these findings to improve full-physics simulations and to evaluate the influence of such energy expenditures on tornado dynamics.

Two aspects of the calculations reported here bear further discussion. First, trees have been modeled individually to the extent possible under the implicit assumption that each tree operates independently from other trees. Since trees in nature can offer one another mutual support, the appropriateness of separately considering the effect of each tree on the wind field remains unclear. Second, unlike the static structures in Lewellen (2014), which addresses the influence of local roughness on the tornadic wind field, trees in a tornado are highly dynamic and their influence on the wind field will change dramatically if the tree is uprooted or broken. Therefore, it is important to emphasize that the drag forces calculated here correspond with a forest prior to any treefall. As a tornado passes, trees will overturn and these interactions will change rapidly. A tornado may encounter short-lived, but substantial, drag-induced effects if it moves across a sharp boundary from a low-roughness surface

into a full-stature forest.

This represents the first attempt to investigate the energy expenditure and mechanical work accomplished by tornadoes passing through heavily-forested landscapes and the associated surface drag induced by a forest. As such, and because of the limitations and constraints of the available observations, this study incorporates a number of assumptions and simplifications. However, the calculations incorporate a substantial amount of realism wherever possible. Future work will undoubtedly examine these underlying assumptions to determine, for example, the appropriateness of a uniform vertical wind profile or whether or not static winching studies produce the most realistic estimates for tree wind resistance (cf. Holland et al. 2006; Beck and Dotzek 2010). Estimates of drag force, torque, and mechanical work accomplished by tornadoes could therefore benefit from potential improvements based on refined input from future research efforts.

*Acknowledgments.* This analysis is funded by NOAA/OAR/NSSL and the VORTEX-SE program through grants NA15OAR459022[7,8,9] and NA16OAR45902[19,20,21] and benefited from data acquired during a project funded by NSF RAPID grants AGS-1141926 and DEB-1143511. The U.S. National Park Service Climate Change Youth Initiative provided additional support.

#### REFERENCES

- Bech, J., M. Gayà, M. Aran, F. Figuerola, J. Amaro, and J. Arús, 2009: Tornado damage analysis of a forest area using site survey observations, radar data and a simple analytical vortex model. *Atmos. Res.*, **93**, 118–130.
- Beck, V., and N. Dotzek, 2010: Reconstruction of near-surface tornado wind fields from forest damage. *J. Appl. Meteor. Climatol.*, **49**, 1517–1537.
- Bosart, L. F., A. Seimon, K. D. LaPenta, and M. J. Dickinson, 2006: Supercell tornadogenesis over complex terrain: The Great Barrington, Massachusetts, tornado on 29 May 1995. *Wea. Forecasting*, **21**, 897–922.
- Brooks, H. E., 2004: On the relationship of tornado path length and width to intensity. *Wea. Forecasting*, **19**, 310–319.
- Burgess, D., and Coauthors, 2014: 20 May 2013 Moore, Oklahoma, tornado: Damage survey and analysis. *Wea. Forecasting*, **29**, 1229–1237.
- Cannon, J. B., 2015: Crash and burn: Forest tornado damage, its landscape pattern, and its interaction with fire. Ph.D. dissertation, University of Georgia, 164 pp.
- Cannon, J. B., M. E. Barrett, and C. J. Peterson, 2015: The effect of species, size, failure mode, and fire-scarring on tree stability. *For. Ecol. Manag.*, **356**, 196–203, doi:10.1016/j.foreco.2015.07.014.
- Cannon, J. B., J. Hepinstall-Cymerman, C. M. Godfrey, and C. J. Peterson, 2016: Landscape-scale patterns of forest tornado damage in mountainous terrain. *Landscape Ecol.*, **31**, 2097–2114, doi:10.1007/s10980-016-0384-8.
- Everham, E. M., III, and N. V. L. Brokaw, 1996: Forest damage and recovery from catastrophic wind. *Bot. Rev.*, **62**, 113–185.
- Forbes, G. S., 1998: Topographic influences on tornadoes in Pennsylvania. Preprints, *19th Conf. on Severe Local Storms*, Minneapolis, MN, Amer. Meteor. Soc., 269–272.
- Godfrey, C. M., and C. J. Peterson, 2016: Estimating enhanced Fujita scale levels based on forest damage severity. *Wea. Forecasting*, in press, doi:10.1175/WAF-D-16-0104.1.
- Holland, A. P., A. J. Riordan, E. C. Franklin, 2006: A simple model for simulating tornado damage in forests. *J. Appl. Meteor. Climatol.*, **45**, 1597–1611.
- Karstens, C. D., W. A. Gallus, B. D. Lee, and C. A. Finley, 2013: Analysis of tornado-induced tree fall using aerial photography from the Joplin, Missouri, and Tuscaloosa–Birmingham, Alabama, Tornadoes of 2011. *J. Appl. Meteor. Climatol.*, **52**, 1049–1068, doi:10.1175/JAMC-D-12-0206.1.
- Kuligowski, E. D., F. T. Lombardo, L. T. Phan, M. L. Levitan, and D. P. Jorgensen, 2014: Technical Investigation of the May 22, 2011, Tornado in Joplin, Missouri. Final Report NIST NCSTAR 3, National Institute of Standards and Technology (NIST), 428 pp.
- LaPenta, K. D., L. F. Bosart, T. J. Galarneau, and M. J. Dickinson, 2005: A multiscale examination of the 31 May 1998 Mechanicville, New York, F3 tornado. *Wea. Forecasting*, **20**, 494–516.
- Letzmann, J. P., 1925: Fortschreitende Luftwirbel (Advancing air vortices). *Meteorol. Z.*, **42**, 41–52.
- Lewellen, D. C., 2012: Effects of topography on tornado dynamics: A simulation study. Preprints, 26th Conference on Severe Local Storms, Nashville, TN, Amer. Meteor. Soc., 4B.1. [Available from <https://ams.confex.com/ams/26SLS/webprogram/Paper211460.html>.]
- Lewellen, D. C., 2014: Local roughness effects on tornado dynamics. Preprints, 27th Conference on Severe Local Storms, Madison, WI, Amer. Meteor. Soc., 15A.1. [Available from <https://ams.confex.com/ams/27SLS/webprogram/Paper254357.html>.]
- Lillesand, T. M., R. W. Kiefer, and J. W. Chipman, 2015: *Remote Sensing and Image Interpretation*. 7th ed. John Wiley & Sons, 736 pp.
- Lyza, A. W., and K. R. Knupp, 2014: An observational analysis of potential terrain influences on tornado behavior. Preprints, 27th Conference on Severe Local Storms, Madison, WI, Amer. Meteor. Soc., 11A.1A. [Available from <https://ams.confex.com/ams/27SLS/webprogram/Paper255844.html>.]
- Markowski, P. M., and N. Dotzek, 2011: A numerical study of the effects of orography on supercells. *Atmos. Res.*, **100**, 457–478.
- Peltola, H., 2006: Mechanical stability of trees under static loads. *Amer. J. Botany*, **93**, 1501–1511.
- Peterson, C. J., 2007: Consistent influence of tree diameter and species on damage in nine eastern North America tornado blow-downs. *For. Ecol. Manag.*, **250**, 96–108.
- Peterson, C. J., and V. Claassen, 2013: An evaluation of the stability of *Quercus lobata* and *Populus fremontii* on river levees assessed using static winching tests. *Forestry*, **86**, 201–209, doi:10.1093/forestry/cps080.
- Roberts, B., M. Xue, A. D. Schenkman, and D. T. Dawson II, 2016: The role of surface drag in tornadogenesis within an idealized supercell simulation. *J. Atmos. Sci.*, **73**, 3371–3395, doi:10.1175/JAS-D-15-0332.1.

Rudnicki, M., U. Silins, V. J. Lieffers, and G. Josi, 2001: Measure of simultaneous tree sways and estimation of crown interactions among a group of trees. *Trees-Struct. Funct.*, **15**, 83–90.

Schenkman, A. D., M. Xue, and M. Hu, 2014: Tornadogenesis in a high-resolution simulation of the 8 May 2003 Oklahoma City supercell. *J. Atmos. Sci.*, **71**, 130–154.

Webb, V. A., M. Rudnicki, and S. K. Muppa., 2013: Analysis of tree sway and crown collisions for managed *Pinus resinosa* in southern Maine. *Forest Ecol. Manage.*, **302**, 193–199.

WSEC, 2006: A recommendation for an enhanced Fujita scale (EF-scale). Texas Tech University Wind Science and Engineering Center Rep., 95 pp. [Available online at [www.depts.ttu.edu/weweb/pubs/fscale/efscale.pdf](http://www.depts.ttu.edu/weweb/pubs/fscale/efscale.pdf).]